IEEE Access
Multidisciplinary | Rapid Review | Open Access Journal

Received March 2, 2022, accepted March 12, 2022, date of publication March 16, 2022, date of current version March 25, 2022.

Digital Object Identifier 10.1109/ACCESS.2022.3160175

A Novel Method to Determine the Handover Threshold Based on Reconfigurable Factor Graph for LEO Satellite Internet Network

WENLIANG LIN[1], YILIE HE[1], KE WANG[2], ZHONG-LIANG DENG[1], (Senior Member, IEEE), DONGDONG WANG[3,4], XIAOYI YU[1], YANG LIU[1], HAO LIU[1], LEI GU[1], AND BINGYU XU[5]

[1]School of Electronic Engineering, Beijing University of Posts and Telecommunications (BUPT), Beijing 100876, China
[2]School of Information and Communication Engineering, Beijing University of Posts and Telecommunications (BUPT), Beijing 100876, China
[3]Academy for Network and Communications, China Electronics Technology Group Corporation (CETC), Shijiazhuang 050081, China
[4]Science and Technology on Communication Networks Laboratory, Shijiazhuang 050081, China
[5]China Academy of Information and Communications Technology, Beijing 100876, China

Corresponding authors: Ke Wang (wangke@bupt.edu.cn) and Wenliang Lin (charterlin@bupt.edu.cn)

This work was supported in part by the China National Key Research and Development Plan under Grant 2020YFB1808005 and Grant 2019YFB1803105, in part by the 13th 5-year plan Civil Aerospace Technology Advance Research Project (D030301), in part by the Hebei Province High-Level Talent Funding Project (B2021003032), in part by the New Technology Research University Cooperation Project (SKX212010010), and in part by the Fundamental Research Funds for the Central Universities.

ABSTRACT Satellite Internet Network (SIN) will be the next heat issue in the ongoing research of 6G. The users need to keep operating handover between different beams or satellites in an extremely high frequency for the satellite to move at high speed in Low Earth Orbit (LEO). Traditional handover thresholds (HT) determined by singer factor (such as reference signal receiving power or quality) have severe performance degradation in the scenarios of SIN. It is also hard to correctly describe and model the correlations between multi factors. This paper proposed a novel method to determine the handover threshold based on a reconfigurable factor graph (FG) for LEO SIN. First, we introduce a tensor to make a factor graph with the ability to reconfigure all the factors and correlations in the factor graph, which can solve the problems of sharp changes between factors. Then, we proposed a method to determine the HT for SIN based on re-constructed FG. The simulations show that the proposed HT method has better performance than those of RSRQ and elevation.

INDEX TERMS LEO satellite, handover, handover threshold, factor graph.

I. INTRODUCTION

One of the scenarios of the Sixth generation (6G) in the recent research is achieved global communications. The key performance indicators (KPI) of 6G would be high-data-rate, low latency, high reliability, and large connectivity density around the world [1]–[3]. Compared to the limited coverage by terrestrial networks, the satellite network would be the first choice to cover most areas on the earth [4], [5]. That would also be a big challenge to achieve all the above KPIs by the traditional satellite network. Therefore, the evolution of satellite internet networks (SIN) has gotten much attention. There are some new characteristics for SIN, such as Low Earth Orbit (LEO) large constellation, Ku/Ka frequency band, and OFDM-based radio.

The satellites in SIN move at an extremely high speed of more than 20000km/h, so the multiple beams of SIN would move at the same high-speed relative to the users on the surface of the earth [6]. To maintain continuous communications in SIN, the users must keep operating handover from one beam or different satellite to the next beam and satellite at an extremely high frequency [7].

High-efficiency handover would play a key role in SIN. Existed handover schemes focus on more accurate offset and hysteresis of the measured values of observed factors, which provide with more stable and higher efficiency handover. In Long term Evolution (LTE) or the fifth-generation (5G), the cell selection criterion S and re-selection criterion R are fulfilled according to the power or the quality of the

The associate editor coordinating the review of this manuscript and approving it for publication was Wei Feng.

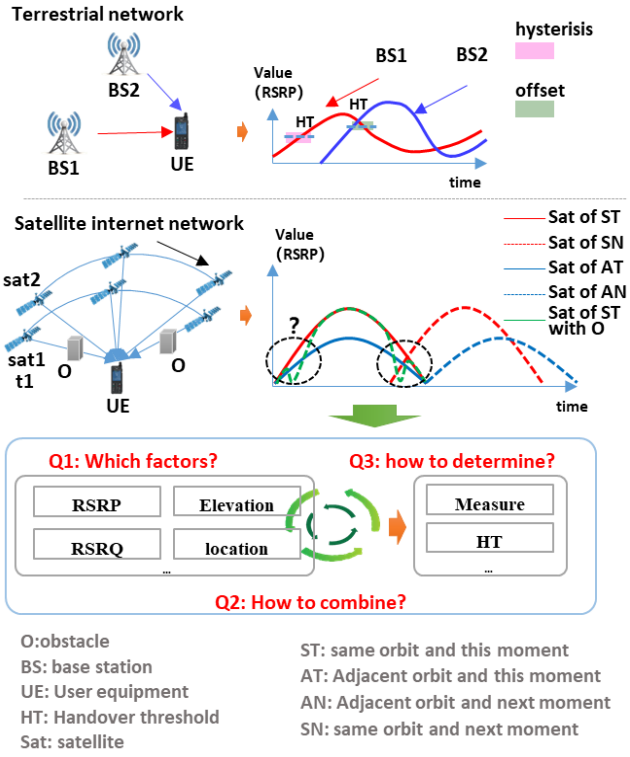

FIGURE 1. The challenges of handover in SIN.

received signal, which are taken as single factors. However, in the scenarios of SIN, the handover schemes with single factors cannot matter since there are multi-affected factors of multi-processes in the determination of handover triggers. Difference in the power of the received signal between center and edge of beams in SIN is near, which is about 3dB. Taking the power of the received signal as the factor of criterion increase the probability of handover failure, which would degrade the Quality of Services (QoS) of SIN. The challenges of handover in SIN are shown in Figure 1.

In Figure 1, there are three questions of handover in SIN,

1) Which factors would be considered in handover schemes: different criterions based on different factors would affect the performance of handover, which include Reference Signal Receiving Power (RSRP), Reference Signal Receiving Quality (RSRQ), the relative distance between user equipment (UE) and satellite (RD), satellite ephemeris (SE), or elevation from UE to the satellite. Which factors would be the most appropriate in different phases and moments?

2) How to combine different factors to determine handover trigger: different factors have different dimensions and different effective ranges. Considered the vision of 5G NR fused with SIN, a unified framework with different factors for handover contributes a lot to minimal protocol changes in the baseband unit.

3) How to operate the process to enhance the efficiency of handover: under the above factors and framework, how and when to measure the values of those factors, how to determine the handover threshold (HT) of each factor and the whole process.

TABLE 1. List of nomenclature.

Acronym	Full Term
SIN	Satellite Internet Network
6G	Sixth Generation Mobile Networks
5G	Fifth Generation Mobile Networks
LEO	Low Earth Orbit
LTE	Long Term Evolution
BS	Base Station
HT	Handover Threshold
QoS	Quality of Services
RSRP	Reference Signal Receiving Power
RSRQ	Reference Signal Receiving Quality
UE	User Equipment
RD	Relation Distance
SE	Satellite Ephemeris
DP	Deciding Process
SFDP	Singer Factor Deciding Process
MFDP	Multi-Factors Deciding Process
CSI	Channel State Information
FG	Factor-Graph
ES	Earth Stations
MS	Monitor Stations
CN	Core Networks
N-C	Network Nodes for Handover Control
NTN	Non-Terrestrial Network
RAN	Radio Access Network
N-U	User Nodes for Handover Control
N-E	Environment for Handover Control
RSSI	Received Signal Strength Indication
HE	Handover Eigenvalues
RRM	Radio Resource Measurement
GNSS	Global Navigation Satellite System
HEM	Handover Eigenvalues Measurement
PDF	Probability Density Function
RFG-T	Re-construct FG based on Tensor
BV	Basis Vectors
AV	Auxiliary Vectors
H-FN	Handover Factor-Node
MAP	Maximum a Posteriori
EA	Elevation Angle
HER	Handover Error Rate

Factor-Graph (FG) schemes can describe the correlations between different factors and sub-factors, so it has an advantage on the HT modeling in the case of one observed factor. To our knowledge, this paper is the first attempt to use FG schemes to model the factors and correlations of HT determination. Although that, FG schemes should be furtherly enhanced, especial for the performance of the handover reliability in the case of multi-observed factors. That means the FG described in one scenario can be extended to describe another scenario. FG should also be re-construct. Therefore, this paper focuses on a new method to determine the HT based on re-constructed FG for SIN. The main contributions are summarized as follows:

a) We build a system model including user model, resource model, channel model, and the satellite in SIN adopts beam hopping technology.

b) We proposed a method to achieve the re-constructed FG for the scenarios with sharp changes, which provided a theoretical basis to determine the HT for SIN;

c) We first proposed a method to determine the HT for SIN based on re-constructed FG, which improves the handover performance in SIN for the scenarios with sharp changes, compared with the methods only considered RSRP or RSRQ.

The remainder of the paper is organized as follows. In Section 2, we conducted research on related work. In Section 3, we demonstrate the system model. The new method to determine the HT for SIN based on the re-construct FG is introduced in Section 4. In Section 5, we introduce the simulations and analyze the performance. Section 6 is the conclusions of the paper.

II. RELATED WORK

Researches on handover schemes focused on Deciding Process (DP), including Singer Factor Deciding Process (SFDP) and Multi-Factors Deciding Process (MFDP). Researchers have identified some factors, such as received power, signal quality, distance, elevation angle, load, etc.

Handover schemes based on RSRP [8]–[11] and RSRQ [12]–[15] are often used in terrestrial communication systems. For example, T. Sheu and J. Sie proposed a dynamic adjustment scheme of handover threshold based on RSRP to balance the load between source BS and target BS [8]. The handover scheme based on RSRP and RSRQ is suitable for the terrestrial network, and the improved handover scheme based on RSRP and RSRQ has better performance, but the handover scheme based on RSRP and RSRQ cannot be applied to the satellite communication system with average beam power.

In the satellite communication system, handover is still a hot issue worth paying attention to. To aim at the characteristics of satellite networks with long time delay and high dynamic, new handover factors are studied, elevation Angle, position, load, and other factors are used in the handover scheme [4], [16]–[26]. A. Bottcher proposed a maximum elevation handover strategy, which always selects the satellite with the best elevation [16]. E. Papapetrou proposed three different satellite handover strategies, namely maximum elevation strategy, maximum visibility strategy, and maximum idle channel strategy, and analyzed the success rate of different handover strategies [17]. C. Duan adopted a location-based minimum-delay handover strategy [4]. T. A. Chowdhury proposed an adaptive channel reservation scheme for switching call priority, allocating resources for switching calls by protecting channels [23]. However, the maximum elevation of the satellite does not necessarily reflect the real link quality, and the location-based handover scheme only considers the minimum delay at the current moment, the handover scheme based on channel reservation only consider the relationship between handover calls and new calls, it is impossible to ensure that the terminal can maintain good communication quality under the service of the target satellite after handover.

Due to the shortcomings of SFDP, recent researches consider the handover schemes for SIN as MFDP, which would

TABLE 2. List of symbols.

Symbol	Meaning
S	Network nodes for handover control
s_{ij}	ith satellite in jth orbits
U	User nodes for handover control
lu_n	nth UE
u_k	Observed UE
$l(t)$	Position of u_k
θ_l	Elevation angle between UE and satellites
$C(t)$	Channels environments between s_{ij} and UE
$eph(t)$	Ephemeris
A	System coverage area
$v(t_i)$	Velocity of UE
$\gamma(t_i)$	Direction of UE
μ_v	Asymptotic mean values of velocity
μ_γ	Asymptotic mean values of direction
t_{step}	The time interval between t_i and t_{i-1}
η_v	Value controls the randomness of the speed
η_γ	Value controls the randomness of the direction
t_c	User's movement time in a complete beam
v_s	Satellite moving speed
m	Number of beams
t_{ca}	Call duration
t_{mc}	The residence time of the source cell,
P_h	Probability of the original call request handover
$t_{mc}^{(k)}$	Time interval from the k-1th handover to the kth handover
$E(i)$	The average number of successful handovers during the entire call duration
$h^{u,l}$	Channel parameter between user u and beam l
$b_{u,l}$	Channel parameter includes multi-beam antenna gain, free space loss, and noise power
Q_u	Channel parameter includes phase and Rain attenuation
G_{re}	Receiving antenna gain
$\chi_u^{-\frac{1}{2}}$	Rain attenuation component
$x_{u,dB}$	Power attenuation
ϕ_u	Uniform random variable
$\Psi_{u,l}$	Free space loss and noise power
λ	wavelength
κTB	The noise component
$G_{u,l}$	Multi-beam antenna gain between user u and the lth spaceborne antenna
$J_1(\cdot)$	The first-order Bessel function of the first kind
$J_3(\cdot)$	The third-order Bessel function of the first kind
α_n	Weight of each factor
G	Factor graph (FG)
F	Local functions in factorization
X	Variables in a global function
f_i	Factor nodes
$g(x_n)$	Function with n variable
$\mu_{f_3\to x_3}(x_3)$	Sum of all variables messages to the left of x_3 in FG
$\mu_{f_4\to x_3}(x_3)$	Sum of all the variables to the right of x_3 in FG
$\mu_{f_5\to x_3}(x_3)$	Sum of all the variables to the right of x_3 in FG
N_i	Number of paths getting in and out the factor-nodes
g_k	A weighted sum of the self-access degree of all factors in the factors cluster
X_k	An estimated value of HT
$h(\cdot)$	Measurement functions of each factor node
Z_k	The actual measurement value of each factor
$L(\cdot)$	Cost functions
$d(\cdot)$	Cost functions
$p(X\|Z)$	Posterior probability density
$\Phi(X)$	A global function that can be factorized into a product of all factors
X^{MAP}	Optimal estimate value of the expected state variable
$\Phi_i(f_j)$	Error probability of the cost function $\Phi(X)$
$X_i(f_j)$	Error probability of each state variable
$X(f)$	probability of HT failure $\frac{N\_nth}{N}$ or $\frac{N\_hto}{N}$
N	Number of all handovers
N_nth	Number of handovers that would not be operated but operated for wrong determinations
N_hto	Number of handovers that would be operated but operated for wrong determinations
$\Delta maxh\_value$	Range of determination of the maximum number of launch handovers maxh_range

determine the HT by two or more factors [19], [27]–[35]. The handover schemes determined by the combination of SE and RSRP can predict which satellites would be at the field of vision around the UE at this moment and next moment. At the same time, the cell selection criterion S based on RSRP can furtherly help select the beam of satellite with appropriate RSRP. The handover schemes by MFDP have enhanced the performance of handover reliability. Fan Zhihui proposed a weighted MFDP based on traffic types, but the algorithm artificially divided network traffic and could not objectively adjust network factors [28]. M Mansouri compares various combinations of MFDP algorithms and proposes a new network selection scheme, which aims to meet the requirements of QoS to the maximum extent [29]. However, MFDP schemes could not furtherly describe the correlations between sub-factors from factors and factors. These would make the HT determined by MFDP schemes fail to be applied in the scenarios with a large area, multi-dimensions, complex scenarios. The high-speed movement between satellites and UEs would bring sharp changes in the correlations to affect the determination of HT.

III. SYSTEM MODEL

According to the position of network nodes, the SIN system can be divided into space segment and ground segment. All satellites are in the space segment. Moreover, there are several earth stations (ES), monitor stations (MS), and core networks (CN), as well as different types of UEs, such as handheld, vehicle-mounted and shipborne terminals [14] in the ground segment. Those network nodes can be abstracted into several categories since they have different functions in SIN handover.

- **Network nodes for handover control (N-C)**: according to the proposals from 5G non-terrestrial network (NTN), the control functions of the radio access network (RAN) can be deployed in the ESs or the satellites. They mainly achieve the functions of message broadcasting, receiving user measurement reports, handover judgment, and data retransmission control.
- **User nodes for handover control (N-U)**: the responding to the handover in the UEs, which achieve channel status measurement, broadcast control message receiving, handover activation, data reception, etc.
- **Environment for handover control (N-E)**: the channels between the satellites and UEs, which would change with the relative distance between satellites and UEs, and services scenarios.
- **The factors of HT determinations**: Received Signal Strength Indication (RSSI) such as RSRP/RSRQ is commonly used in existing terrestrial mobile communication systems. The factors such as ephemeris, elevation angle, the position should also be considered.

The system model of SIN includes the user model, resource model, channel model, as shown in Figure 2.

There are several satellites in the network framework of SIN. The beams of satellites move with a footprint on the earth with a specific coverage, speed, or direction according to the constellations and orbits. The network nodes for handover control are denoted as $S = \{s_{11}, s_{12}, \ldots, s_{ij}\}$, which is composed of $i * j$ satellites, i is the number of orbits, j is the number of satellites in the orbits, s_{ij} is the ith satellite in ith orbits. Because the functions of access control can be placed in satellites or ESs, we take the satellite or ESs as the same network nodes.

The handover of users' links is the most concerning issue in this paper. We assume the observed UE is u_k, which denotes the kth UE. The position of u_k is $l(t)$, which would change with time. Here, we assume that the u_k would access to the satellite s_l, the elevation angle between UE and satellites θ_l is about $\{45°, 135°\}$. At this moment, the elevation angle θ_{l-1} of the previous satellites which the u_k access is about $\{0°, 45°\}$, the elevation angle θ_{l+1} of the next satellite s_{l+1} which the u_k access is about $\{135°, 180°\}$. Here, we define the elevation range as $\{0°, 180°\}$. The elevation angles θ_l, θ_{l-1}, θ_{l+1} are all considered the UEs are in the center of the beams of satellite s_l. The elevation angle is calculated from the satellite position and the UE position. The UE stores the basic orbital plane parameters and broadcasts the orbital parameters of the serving satellite in the system information. The UE derives the position coordinates of the serving satellite accordingly. The ephemeris data of the neighboring satellites can also be provided to the UE through system information or dedicated RRC signals. The channels environments between s_{ij} and UE U are denoted as $C(t)$, which are a set of factors such as $rsrp(t)$, $rsrq(t)$, $C(t)$, $eph(t)$, $\theta_l(t)$, etc. We illustr iders RSRP and serving time, as shown in Figure 3, and the service satellite is denoted as S1, adjacent orbit satellite is denoted as S2. Since different factors have various degrees of influence in handover processes, HT should be considered in stages. When the RSRP difference is not apparent, this factor cannot be used as a handover decision factor. When the serving time of all satellites is less than the threshold, the handover scheme cannot effectively select the target satellite.

To study and simulate various influencing factors in MFDP and build a simulation platform, we established user model, resource model, and channel model, respectively.

A. USER MODEL

The user model includes the user distribution model, traffic model, and mobility model. The user distribution in this paper adopts sparse and uniform distribution, set the coverage area as A, the user coordinate as (x, y), and the system coverage area as $Area$, then the probability density function can be expressed as

$$f(x) = \begin{cases} \frac{1}{A}, & (x, y) \in Area \\ 0, & (x, y) \notin Area \end{cases} \quad (1)$$

The global traffic arrival rate follows a Poisson distribution with an average value of 5000/s, and the ses-

TABLE 3. The comparisons of the related work.

Papers	Years	Factors	The concerned topics	The key problem
[8]	2018	RSRP	Dynamically adjustable handover threshold	Distinguish the state of the UE according to the RSRP strength, and calculate the handover factor adjustment threshold
[9]	2021		Handover parameter optimization	Two-step clustering completes the classification of UE regions and optimizes handover parameters for different regions respectively
[10]	2007		Handover algorithm with trigger time window	Study the effect of trigger window size on handover performance
[11]	2019		Adaptive RSRP-based threshold	Research on the design of adaptive RSRP threshold formula for UE mobility
[12]	2014	RSRQ	Adaptive pre-switch algorithm	Predict user's movement based on Gauss-Markov mobility model to assist handover decision
[13]	2015		Heterogeneous network	Performance comparison of RSRP and RSRQ based-handover in heterogeneous networks
[14]	2008		Handover performance evaluation	Evaluating the applicability of RSRQ-based measurements in inter-frequency handovers
[15]	2010		Adaptive time window	Definition and Design of Adaptive Time Window
[16]	1994	EA	Handover decision based on elevation	Selection of the best elevation angle
[17]	2003		Comparison of satellite handover strategies	Analysis and comparison of maximum elevation angle strategy, maximum visibility strategy, and maximum clear channel strategy
[18]	2001		Channel-assisted adaptive handover scheme	The signal intensity related to elevation angle is used as the handover criterion
[19]	2004	Position	Handover decisions based on user location	Handover decision based on user location and communication distance
[4]	2018		Decisions based on location information of both parties	Based on location information, a strategy that considers the least delay
[20]	1996		A handover algorithm that considers the user's location	Position estimation by measuring the transmission of packets
[21]	2019		Positioning Based Intra-Frequency Handover	Predict position coordinates and map to RSRP values for handover decisions
[22]	2018		Handover in high-speed trains	Handover decisions based on train location, direction, and base station deployment
[23]	2014	Load	Adaptive channel reservation scheme	Design of variable protection channel based on channel occupancy
[24]	2015		The optimal number of channels reserved	Establish the relationship between QoS constraints and maximum flow, and derive the expression of maximum flow intensity
[25]	2002		Dynamic call admission policy	Dynamically adjust the total number of new calls accepted by random numbers according to channel occupancy
[26]	1973		Channel borrowing handover scheme	Design of handover process based on channel borrowing
[27]	2019	Multi-factor	Machine learning-based handover	Set up neural network prediction system with which the handover decision parameters like RSRP and RSRQ
[28]	2020		Individualistic dynamic handover parameter self-optimization algorithm	Build a weight function for the three factors, and use the weight function to estimate the handover control parameter settings for optimization
[29]	2018		QoS handover scheme with priorities	Handover decision based on traffic type and data rate allocation priority
[30]	2015		user-behavior based handover	Classify by RSRP, speed, and traffic, and then optimize the handover parameters

sion time is subject to a Pareto distribution with a scale of 7, a shape of 0.5, and a minimum session duration of 30 s [36].

In this paper, the Gaussian-Markov mobility model is used to generate user trajectories in real motion scenes [37]. In this model, velocity $v(t_i)$ and direction $\gamma(t_i)$ are expressed as follows

$$v(t_i) = \eta_v v(t_{i-1}) + (1-\eta_v)\mu_v + X_{i-1}\sqrt{1-\eta_v^2} \quad (2)$$

$$\gamma(t_i) = \eta_\gamma \gamma(t_{i-1}) + (1-\eta_\gamma)\mu_\gamma + Y_{i-1}\sqrt{1-\eta_\gamma^2} \quad (3)$$

where, $i = 1, 2\ldots$, the time interval $t_{step} = t_i - t_{i-1}$, μ_v and μ_γ are the asymptotic mean values of velocity and direction respectively, X and Y are Gaussian processes with mean 0, and the standard deviations of X and Y are the same as those of variables v and γ. The parameter $\eta_{v/\gamma} \in [0, 1]$ controls the randomness of the speed and direction. Take $v(t_i)$ as an example, when $\eta_v = 0$, $v(t_i) = \mu_v + X_{i-1}$, the speed is determined by the asymptotic mean μ_v and the Gaussian random process X_{i-1}, at which time the motion is completely random. When $\eta_v = 1$, $v(t_i) = v(t_{i-1})$, the speed $v(t_i)$ at time t_i is the same as the speed $v(t_{i-1})$ at time t_{i-1}, which means that t_i has nothing to do with time. When $0 < \eta_v < 1$, the factors that affect the speed at the time t_i include: the speed $v(t_{i-1})$ at the last moment, and the control parameters of Gaussian random passing, a total of two factors, as the parameter η_v continues to increase from 0 to 1, $v(t_i)$ is easily affected by the velocity $v(t_{i-1})$ at the last moment; on the contrary, as η_v decreases from 1 to 0, $v(t_i)$ is more susceptible to Gaussian randomness The effect of the process

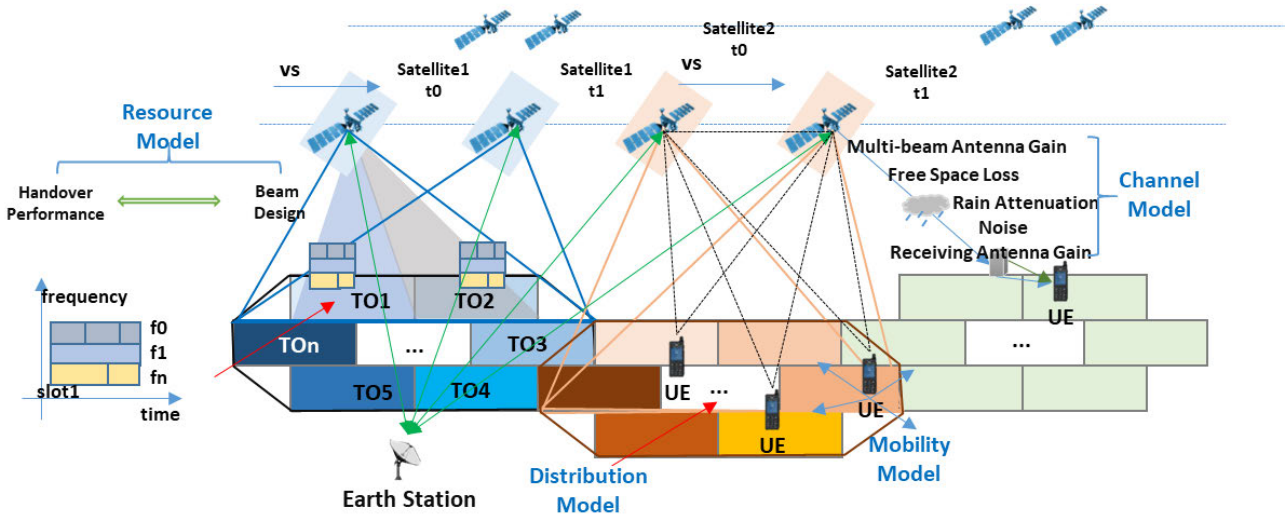

FIGURE 2. System model.

X_{i-1}. Therefore, when $0 < \eta_v < 1$, the randomness of the motion is at an intermediate random level.

B. RESOURCE MODEL

During system modeling, we use circular beams. To achieve seamless coverage, beams need to overlap. When the overlapping area between beams is increased, the system capacity will be improved, but as the overlapping area becomes larger, it will also bring problems such as waste of resources and frequent handovers to the system. We use a regular hexagon circumscribed circle, at this time, the overlapping area is 0.21 times the total area. At the same time, the number of beams will also impact the handover performance. The more spot beams, the more frequent handovers between beams will occur, resulting in much signaling overhead. However, if there are too few spot beams, the reduced system capacity will also affect the handover failure rate.

To simplify the analysis, and inscribed square of a circular beam is taken as an example to illustrate the influence of the number of beams on handover [38]. Assuming that the satellite coverage area is A, the number of beams is m, v_s is the satellite moving speed, and t_c is the user's movement time in a complete beam

$$t_c = \frac{\sqrt{0.79 \cdot A}/\sqrt{m}}{v_s} \tag{4}$$

Assuming that the call duration t_{ca} follows a negative exponential distribution with the mean value of $1/\mu$, and t_{mc} is the residence time of the source cell, the probability of the original call request handover P_h is

$$P_h = P\{t_{ca} > t_{mc}\} = \int_0^\infty P\{t_{ca} > t | t_{mc} = t\} \cdot f_{t_{mc}}(t)dt \tag{5}$$

Define $t_{mc}^{(k)}$ to represent the time interval from the k-1th handover to the kth handover, and $t_{mc}^{(k)}$ is independent and identically distributed. When a cell undergoes a successful inter-beam handover, the remaining duration also obeys an exponential distribution with a parameter of $1/\mu$. The probability of another handover for the call is

$$\begin{aligned} P_h^{(2)} &= P_h^{(3)} = \cdots = P_h^{(k)} = P_{hk} = P\left\{t_{rca} > t_{mc}^{(k)}\right\} \\ &= \int_0^\infty P\{t_{rca} > t | t_{mc}^{(k)} = t\} \cdot f_{t_{mc}^{(k)}}(t)dt \end{aligned} \tag{6}$$

When the user distribution characteristics are not considered, $t_{mc}^{(k)} = t_c$. Assuming that the new call blocking rate and the handover failure rate are 0, the average number of successful handovers during the entire call duration is

$$E(i) \geq \frac{P_{h1}}{(1 - P_{hk})} = \frac{1 - e^{-t_c\mu}}{t_c\mu\left(1 - e^{-t_c\mu}\right)} = \frac{1}{t_c\mu} \tag{7}$$

The average number of handovers is related to the satellite coverage, beams, and the satellite speed [39], [40]. When the coverage and speed are constant, the more beams, the larger the lower bound of the average number of handovers.

C. CHANNEL MODEL

A satellite channel model is established taking into account atmospheric fading, free space loss, and beam radiation patterns. The channel parameter $h^{u,l}$ from the user, u to beam l can be expressed as

$$h^{u,l} = b_{u,l} \cdot Q_u = \sqrt{\Psi_{u,l} \cdot G_{u,l} \cdot G_{re}} \cdot \chi_u^{-\frac{1}{2}} e^{-j\phi_u} \tag{8}$$

where, $b_{u,l}$ contains the multi-beam antenna gain between user u and the lth spaceborne antenna, free space loss and noise power, the receiving antenna gain, and Q_u represents the phase and rain attenuation variation. Among them, G_{re} is the receiving antenna gain, $\chi_u^{-\frac{1}{2}}$ is the rain attenuation component, $x_{u,dB} = 20\log_{10}(x_u)$ represents the power attenuation

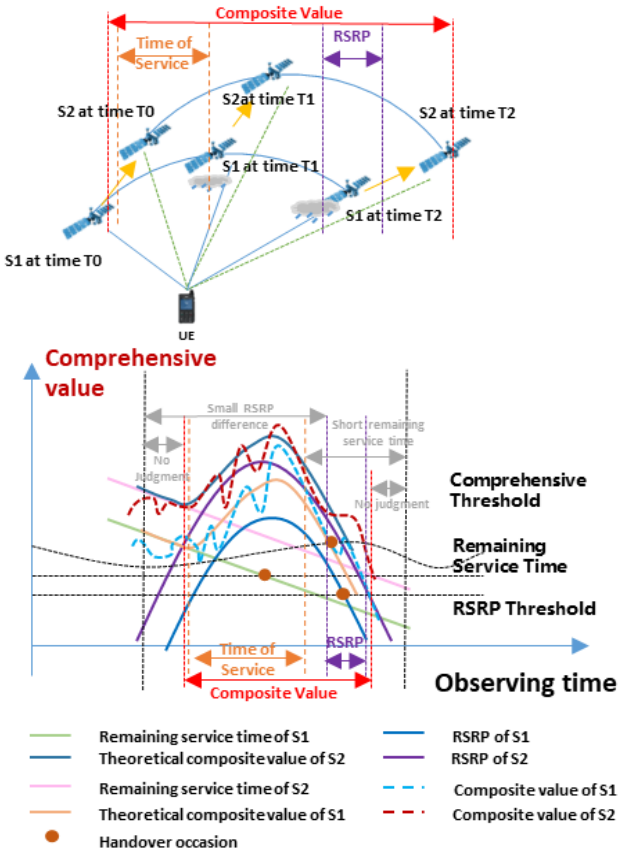

FIGURE 3. MFDP for HT in SIN.

due to rain attenuation, which is usually modeled as a log-normal random variable, i.e. $\ln x_{u,dB} \sim N(\mu, \sigma)$. And $e^{-j\phi_u}$ represents the signal phase, ϕ_u is a uniform random variable within $(0, 2\pi)$.

$\Psi_{u,l}$ is the free space loss and noise power.

$$\Psi_{u,l} = \left(\frac{1}{4\pi \cdot d \cdot \lambda^{-1}}\right)^2 \cdot \frac{1}{\kappa TB} \tag{9}$$

As the propagation distance increases, the energy of the signal will continue to spread, so the free space loss $(1/(4\pi \cdot d \cdot \lambda^{-1}))^2$ can be used to simulate this impact, where d is the distance between the satellite and the user, λ is the wavelength, c is the speed of light, f is the frequency, κTB represents the noise component, where T is the receiver noise temperature, the Boltzmann constant is denoted by κ, and B is the system bandwidth.

$G_{u,l}$ is the multi-beam antenna gain between user u and the lth spaceborne antenna

$$G_{u,l} = G_{max}\left(\frac{J_1(\delta)}{2\delta} + 36\frac{J_3(\delta)}{\delta^3}\right)^2 \tag{10}$$

In the formula, $J_1(\cdot)$ is the first-order Bessel function of the first kind, and $J_3(\cdot)$ is the third-order Bessel function of the first kind. $\delta = 2.07123 \sin(\theta_{u,l}) / \sin(\theta_{3dB,l})$, $\theta_{u,l}$ is the angle between the beam center of beam l and the connection between user u and the satellite, respectively.

IV. A NEW METHOD TO DETERMINE THE HT BASED ON RE-CONSTRUCT FG

To improve the handover performance in SIN, we propose a new method to determine the HT based on re-construct FG. First, FG would be introduced to model the factors, sub-factors, and their correlations by FG. The indicator is constructed to evaluate the weights of each factor's effect on the overall handover efficiency. Second, the cross-dimensional correlations between cross factors are described with a tensor. The FG can be re-construct to solve the problems of sudden correlations weighted changes by the highly changeable environment. At last, a method to determine a suitable HT for SIN based on is proposed based on the re-construct FG.

A. FG OF HT FOR SIN

FG is a dichotomous graph model, denoted as $G = (F, X, E)$. In the model of FG, there are two types of nodes. The first kind of them is factor nodes $f_i \in F$, which are local functions in factorization. The second kind of them is variable nodes $x_i \in X$, which are the variables in a global function. In the edge $e_{ij} \in E$, there is a connecting edge e_{ij} between the variable nodes x_j in FG if and only if they are the independent variables of the corresponding factor nodes f_i. The primary purpose of FG modeling is to factorize complex correlations of systems.

The sum-product algorithm is based on a message-passing mechanism through the topology of FG, which can accelerate solution procedure with marginal probability [42], [43]. Assume $g(x_n)$ is a function with n variables, if it can be decomposable as [41], [42],

$$\begin{aligned} &g(x_1, x_2, x_3, x_4, x_5, \ldots, x_m, x_n) \\ &\quad = f_1(x_1) \times f_2(x_2) \times f_3(x_1, x_2, x_3) \times f_4(x_3, x_4) \\ &\qquad \times f_5(x_3, x_5) \times \ldots \times f_m(x_m, \ldots) \times f_n(x_n, \ldots) \end{aligned} \tag{11}$$

Then (11) can be represented by FG, as shown in Figure 4.

In Figure 4, for example, the marginal probability of the random variable x_3 can be expressed as

$$g(x_3) = \mu_{f_3 \to x_3}(x_3) \cdot \mu_{f_4 \to x_3}(x_3) \cdot \mu_{f_5 \to x_3}(x_3) \tag{12}$$

where, $\mu_{f_3 \to x_3}(x_3)$ is the sum of all variable messages to the left of x_3 in FG. $\mu_{f_4 \to x_3}(x_3)$ and $\mu_{f_5 \to x_3}(x_3)$ are the sum of all the variables to the right of x_3 in FG.

$\mu_{f_3 \to x_3}(x_3)$ can be expanded as follows,

$$\begin{aligned} \mu_{f_3 \to x_3}(x_3) = \sum\nolimits_{\sim\{x_3\}} &\left[f_3(x_1, x_2, x_3) \cdot \mu_{x_1 \to f_3}(x_1)\right. \\ &\left. \cdot \mu_{x_2 \to f_3}(x_2)\right] \end{aligned} \tag{13}$$

$\mu_{f_m \to x_{m-1}}(x_{m-1})$ and $\mu_{f_n \to x_{n-1}}(x_{n-1})$ can be expanded as follows,

$$\mu_{f_m \to x_{m-1}}(x_{m-1}) = \sum\nolimits_{\sim\{x_{m-1}\}} f_m(x_m, x_{m-1}) \cdot \mu_{x_m \to f_m}(x_m) \tag{14}$$

$$\mu_{f_n \to x_{n-1}}(x_{n-1}) = \sum\nolimits_{\sim\{x_{n-1}\}} f_n(x_n, x_{n-1}) \cdot \mu_{x_n \to f_n}(x_n) \tag{15}$$

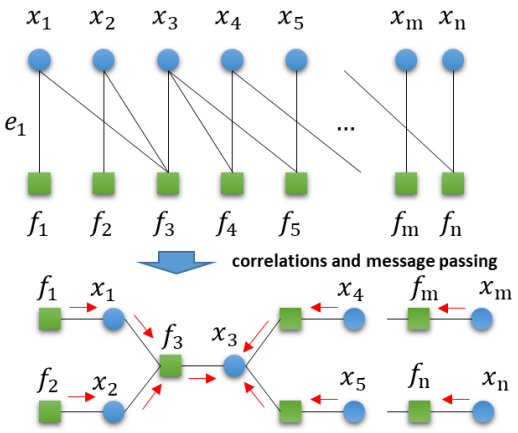

FIGURE 4. The correlations and message passing between factors and sub-factors.

where, $\mu_{x_m \to f_m}(x_m) = 1$, $\mu_{x_n \to f_n}(x_n) = 1$. After the marginal probability of unknown states variables has been obtained by FG, the value of the unknown state variable would be evaluated when the marginal probability gets the maximum.

In this paper, there are various possible components of HT in SIN, the actual situation depends on the handover scenario. We provide the corresponding relationship between FG and HT. The original HT is illustrated in Fig. 5(a), when the handover scenario is changed, FG should update subsequently. Fig. 5(b) shows the situation when the weight of sub-HT changed, and the change of the corresponding FG. Fig. 5(c) is an example when a new sub-HT has been added. Fig. 5(d) is the case when sub-HT split into several sub-HT. Fig. 5(e) illustrates the exchange of sub-HTs.

B. RE-CONSTRUCT FG BASED ON TENSOR (RFG-T)

The severe changes of the scenarios would cause mass changes of factors and those correlations. The previous correlations by fixed and one-dimensional FG cannot describe these sudden changeable correlations. Therefore, to improve the performance of handover, we evaluate affections degree on handover by different dimensions of each factor, then cross-dimensions correlations can be realized by tensor to solve the problems of rapid FG re-constructions.

Re-construct FG based on tensor (RFG-T) includes four steps: modeling unified affections degree of factors, analysis of correlation degree between handover factors, reconstruction correlations between changeable factors, and modeling new FG for handover, as shown in Figure 6.

- **Step1. Modeling unified affections degree of factors:** We set the affections degree evaluation of FG δ_i, $i \in 0, \ldots, M$, where M is the number of factors. The affections degree of each factor is positively related to the access degree of the factor cluster in which the factor is located. The self-access degree N_i, $i \in 0, \ldots, M$ is the number of paths getting in and out the factor-nodes. Here, the access degree of the factors cluster $g_k = (F_k, X_k, E_k)$ would be a weighted sum of the self-access degree of all factors in the factors cluster. Assume that the independent factors determination threshold is N_t, if the access degrees of two factors clusters are close, that is, the access degrees of factor clusters is less than N_t, then the correlation $e_{i,j}$ between factor, clusters would be eliminated.
- **Step2. Analysis of correlation degree between handover factors:** HT is the main factor-node. We sort other factor-nodes by the access degree directly linked to the main factor-node. The different access degrees to different nodes have different weights. The factors with high direct access degrees are defined as the passive protected nodes.
- **Step3. Reconstruction correlations between changeable factors:** As shown in Figure 7, we use a tensor to describe correlations between factors and sub-factors. In multi-dimensions space, determine the node location and connect nodes. The correlations between a factor and the main factor-node are assumed as basis vectors (BV), then, the correlations between a factor and other factor-node are assumed as auxiliary vectors (AV). The weights influenced by correlation degree between different nodes are assumed as the tensor component, then the distances of vectors of the tensor are calculated.
- **Step4. Modeling FG-T for handover:** When the factors and correlations of RFG-T change, the main factor-node of FG would not change, the unchanged factors-node and correlations would also not change. So, we focus on the changed factors-nodes, which first judge whether correlate with the main factor-node. Then, we compare whether the new combinations of vector and component of passive protection nodes are like the old ones. If they are similar, the factor cluster of passive protection nodes makes a direct and new correlation with the main factor-node, then updates the RFG-T. If there is a big difference between them, the observed correlations of a current node would be delivered to the secondary nodes (sub-factors), then compare whether the new combinations of vector and component of passive protection nodes are like the old one again. If they are similar, update the RFG-T. If there is still a big difference between them, we do the above operations again until we model proper RFG-T.

C. HT DETERMINATION BASED ON RFG-T

We construct an RFG-T to consider multi-factors from different dimensions, which model the determination factors and their correlations of HT. The proper value of HT can be solved by the RFG-T.

The procedure of HT determination by RFG-T is described as follows.

We set the factor of handover as the main factor-node and model unified affections degree of factors for handover, that is handover factor-node (H-FN). In this step, we calculate

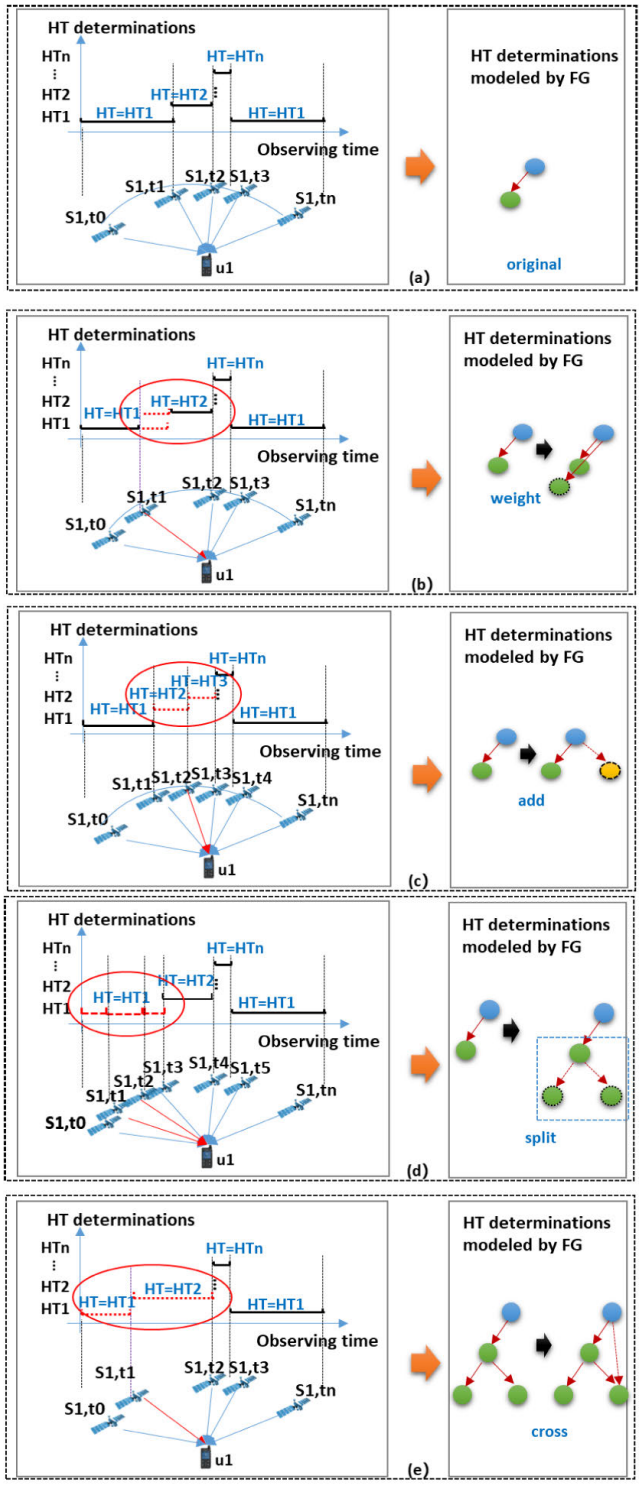

FIGURE 5. Different FGs for HT in different scenarios.

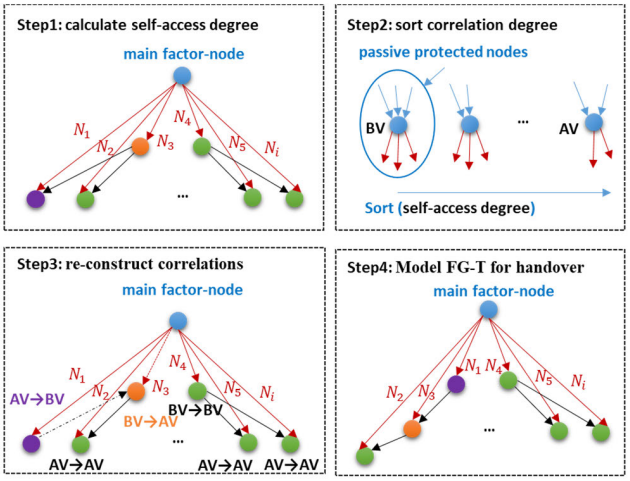

FIGURE 6. Description of FG reconstruction process.

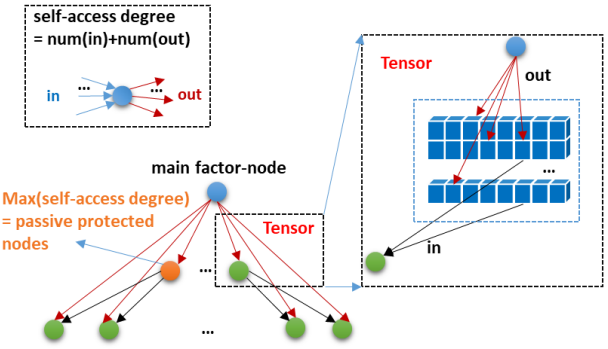

FIGURE 7. Re-construct FG based on tensor.

the self-access degrees of each factor-node and each factor cluster. Then, the correlations between different factors and t H-FN are analyzed. We sort other factor-nodes by the access degree directly linked to H-FN. The weights of correlations with different factors are calculated according to the direct access degree. The factors with a high direct access degree are defined as the passive protection nodes for H-FN. Passive protection nodes include RSRP, RSRQ, distances between satellites and UEs, elevation angle, service time, and QoS. Then we model the correlations between sub-factors from the above passive protection nodes. The correlations between each factor and H-FN have exploited a tensor with vectors sets. We can also gain the BV and AV in RFG-T. The components of vectors can be set by the corrections weight obtained previously. After that, when factors in RFG-T change, we can judge deviations between the tensor vectors and direct access degree, which operate the update RFG-T.

We illustrate RFG-T for handover in the case of Figure 8. In Figure 8, we define circular nodes as variables nodes, rectangular as factors nodes. The factors considered are channel status, service time, atmospheric attenuation, relative distance, doppler frequency offset, multipath attenuation, ephemeris, elevation angle, service, and others. Factors are divided into three categories, including satellites, UEs, and channels. We build a multidimensional space, place all of the factors, namely variables nodes to the multidimensional space. The tensor is constructed according to the relationship

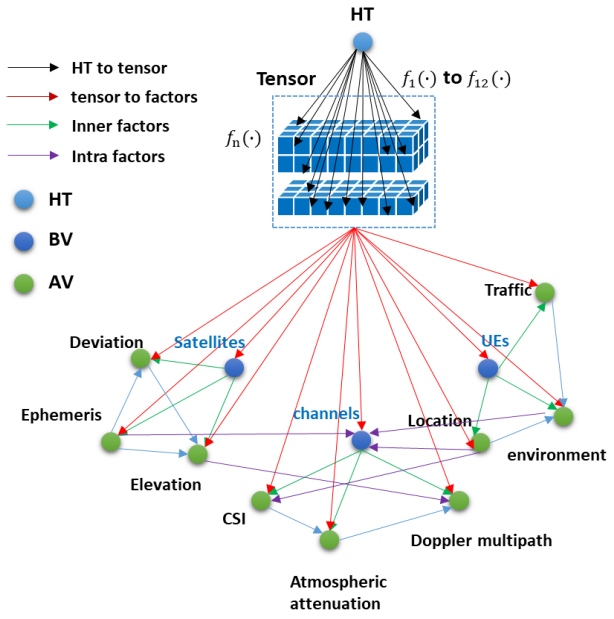

FIGURE 8. Example of HT determination based on RFG-T.

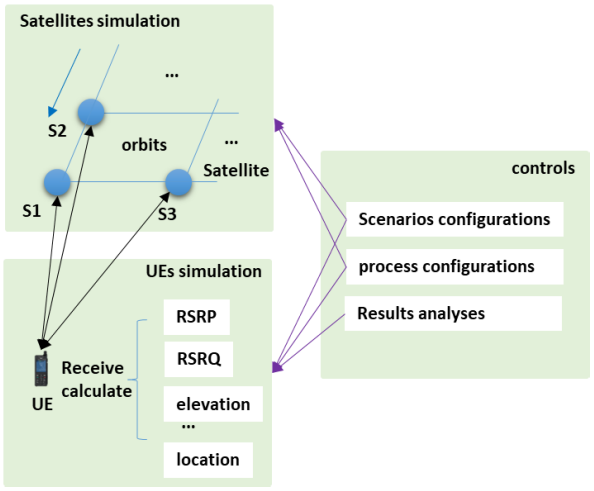

FIGURE 9. A framework of simulation scenario.

between nodes, and the tensor is used in subsequent reconstructions.

In the RFG-T for HT, the factor nodes that have direct correlations with H-FN are expressed as $f(X_k) = L(Z_k - h(X_k))$, Where, X_k is an estimated value of HT, $h(\cdot)$ is the measurement functions of each factor node, Z_k is the actual measurement value of each factor, $L(\cdot)$ is the cost functions. Similarly, the factor nodes between each other can be expressed as $g(X_k) = d(Z_k - h(X_k))$, $d(\cdot)$ is the cost function.

We assume that the handovers happen in Gaussian noise channels, the cost function can usually be further defined as

$$\Phi_i(X_j) = d\left(h_i(X_j) - z_j\right) = e^{-\frac{1}{2}\|h_i(X_j) - z_j\|^2} \quad (16)$$

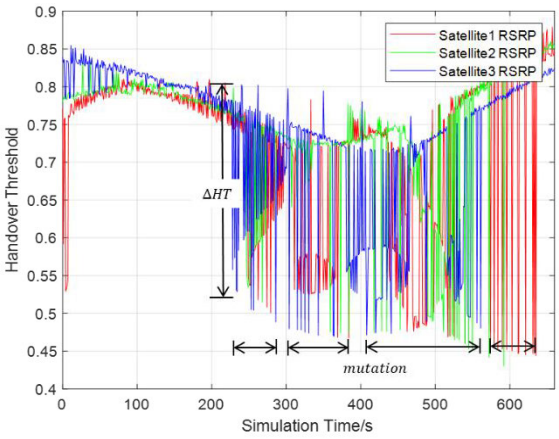

FIGURE 10. Stability of measured values for HT by RSRQ.

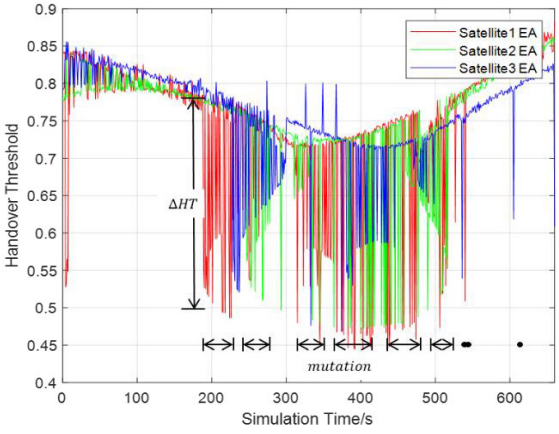

FIGURE 11. Stability of measured values for HT by elevation.

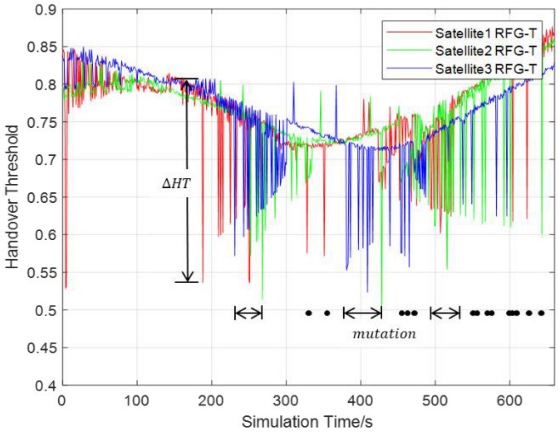

FIGURE 12. Stability of measured values for HT by RFG-T.

where i denotes different factor nodes, j denotes different variable nodes. In this RFG-T, given the measured value z_j, we exploit maximum a posteriori (MAP) estimation to

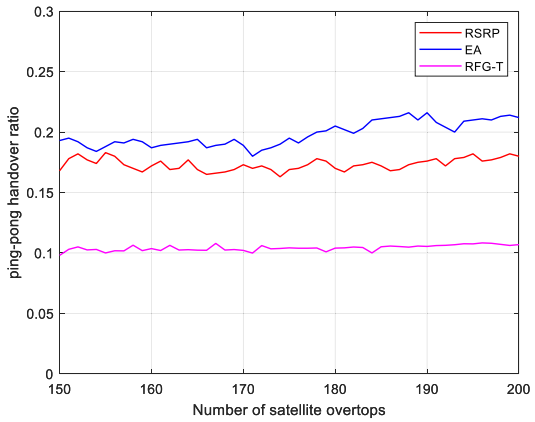

FIGURE 13. Ping-pong handover rates of three handover schemes.

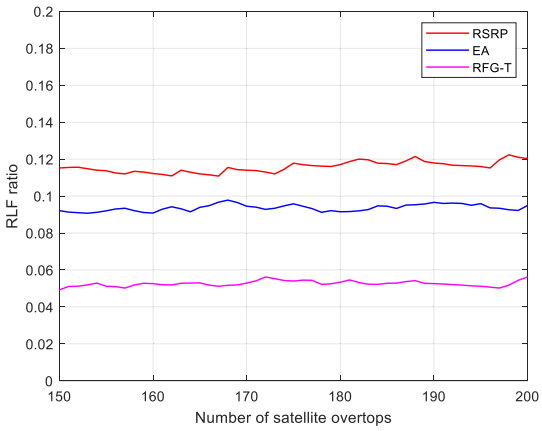

FIGURE 14. Radio link failure rates of three handover schemes.

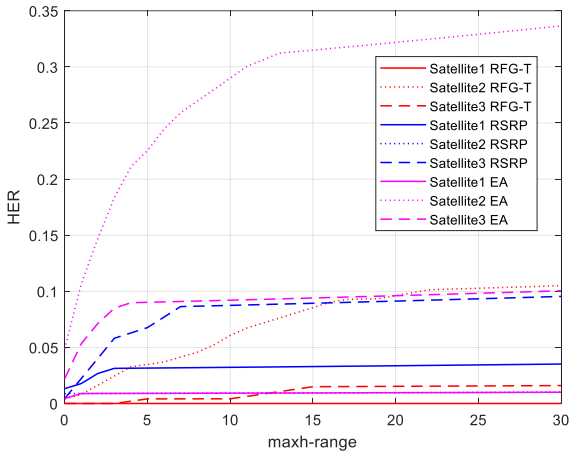

FIGURE 15. Excessive handovers under different handover tolerance value.

solve the probability estimation problem of the unknown state variable (HT). We can get the solutions when the posterior probability density $p(X \mid Z)$ of the state variables get the

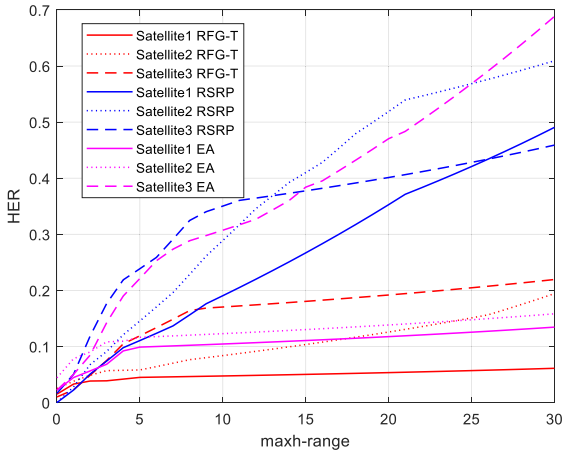

FIGURE 16. Wrong handovers under different handover tolerance value.

maximum value,

$$X^{MAP} = argmaxP(X|Z) \tag{17}$$

For any FG, the MAP (maximum a posteriori) inference boils down to maximizing the product of all factors [43]

$$X^{MAP} = argmax[\Phi(X)] = argmax \prod\nolimits_i [\Phi_i(X_j)] \tag{18}$$

In (18), $\Phi(X) = \prod_i[\Phi_i(X_j)]$ is a global function that can be factorized into a product of all factors. X^{MAP} is the optimal estimate value of the expected state variable. When the $X = X^{MAP}$ is satisfied, the maximum value of $\Phi(X)$ would be obtained. That is, we get the solutions of MAP estimations. In the estimations, we substitute the cost function in (18). Since $h_i(X_j)$ is generally a nonlinear function, we set the initial value of it, then the solution of HT can be solved by the method of Gauss-Newton.

Therefore, the HT in the case of multi-factors affections can be described as,

$$X^{MAP} = argmax[\Phi(X)] = argmax \prod\nolimits_i [\alpha_i \cdot \Phi_i(X_j)] \tag{19}$$

Assume that the error probability of each cost function is $\Phi_i(f_j)$, the error probability of the cost function $\Phi(X)$ is $\Phi(f) = \prod_i[\alpha_i \cdot \Phi_i(f_j)]$.

If the error probability of each state variable is $X_i(f_j)$, the probability of HT failure is $X(f) = \prod_i[X_i(f_j)]$. It has no concern with the weight of each influencing factor. The rate of HT failure would fluctuate less.

V. SIMULATION AND ANALYSIS

A. SIMULATION SCENARIOS

In the simulations, we built scenarios with a permanent UE and three satellites, as shown in Fig. 9. The location of the observed UE is configured in Beijing. Two satellites are in the same orbit with a height of 1100km, the third satellite is in an adjacent orbit at the same height. To see more satellites at the same time and provide more switching options, this article selects the user's minimum elevation angle to the satellite as 1°. Meanwhile, the elevation angle range during the satellite

TABLE 4. Parameters of satellite.

Parameter	Satellite 1	Satellite 2	Satellite 3
Altitude	7471km	7471km	7471km
Eccentricity	0.2833	0.2833	0.2833
First Elevation	7.666°	5.569°	1°
Last Elevation	179°	179°	162.684°
Transmitting Power	45dBm	45dBm	45dBm
Antenna Gain	50dBi	50dBi	50dBi
Carrier Frequency	4GHz	4GHz	4GHz
Number Of Channels	500	500	500
Speed	6.94km/s	6.94km/s	6.94km/s

overhead is set as [0°, 180°]. The parameters of the satellite are configured as follows.

The value of the HT feature is set to demonstrate the results of RRM with different factors. We chose the methods of RSRQ and elevation angle as the reference to compare with the performance of the proposed HT by RFG-T. For example, RSRQ is the value of the HT feature which would be observed in the methods of HT determination by RSRQ.

B. STABILITY OF MEASURED VALUES FOR HT

We first analyze the stability of measured values for HT by different methods. Here, the stability of measured values is the difference between a measured value and expected value from the preset process of UE access to a satellite. The better stability of measured values for HT means more accuracy for the chosen HT. At the beginning of a simulation, satellite 1 is in the orbit of the top of UE, the first observed elevation of satellite 1 is 7.66°, last observed elevation of satellite 1 is 180°. Then, satellite 2 is in the adjacent orbit of the orbit of satellite 1, the first observed elevation of satellite 2 is 5.569°, last observed elevation of satellite 1 is 180°. Satellite 3 is in the adjacent orbit of satellite 1, the first observed elevation of satellite 3 is 0°, last observed elevation of satellite 1 is 162.684°. In this simulation, UE is expected to access from satellite 1 to satellite 3. We observed RSRQ and elevation and factors by MFDP determined by RFG-T.

Figure 10 shows the stability of HT with the method based on RSRP. Figure 11 indicates the stability of HT with the method based on elevation angle (EA). Figure 12 illustrates the stability of RFG-T based HT in the handover process.

In Figure 10 and Figure 11, we can figure out the stability of measured values for HT by RSRP and elevation have more and bigger down peaks in the observation of satellite 1, satellite 2, and satellite 3. Figures 10 to 12, show the number of down peaks in RFG-T based HT is smaller than that of the other two measured values. ΔHT in RFG-T based HT is far less than the other two, and the mutations in RFG-T based HT are sparser than either RSRP based HT or EA based HT.

Figure 10 shows the stability of HT with the method based on RSRP. Figure 11 indicates the stability of HT with the method based on elevation angle (EA). Figure 12 illustrates the stability of RFG-T based HT in the handover process.

In Figure 10 and Figure 11, we can figure out the stability of measured values for HT by RSRP and elevation have more and bigger down peaks in the observation of satellite 1, satellite 2, and satellite 3. Figures 10 to 12, show that the number of down peaks in RFG-T based HT is smaller than that of the other two measured values. ΔHT in RFG-T based HT is far less than the other two, and the mutations in RFG-T based HT are sparser than either RSRP based HT or EA based HT. At the beginning of the simulation, it shows more stability of measured values of satellite 1 than satellite 2 and satellite 3. That is because the observed elevation from UE to satellite 1 is bigger than satellite 2 and Satellite 3. After the observed elevation from UE to satellite 1 is bigger than 135°, the stability of measured values of satellite 3 is more than those of satellite 1 and satellite 2. The UE would hand over and access to satellite 3. In conclusion, it shows the proposed RFG-T method has better performance of stability of measured values than methods of HT determination by RSRQ and elevation. We can avoid unnecessary handovers for the factor of sudden change or measurement error.

C. PERFORMANCE OF HANDOVER BY DIFFERENT HT

In the simulation, if UE handover from satellite 1 to satellite 3 and then handover back to satellite 1, it means that a ping-pong handover has occurred. Set satellite 1 and satellite 3 to pass the UE multiple times. The ratio of the number of ping-pong handovers to the total number of handovers is the ping-pong handover rate. The simulation result graph should take the number of times as the horizontal axis and the ping-pong rate as the vertical axis.

Analyzing the ping-pong handover ratio shown in Figure 13, it can be seen that the handover decision algorithm based on different factors exhibits different performances in ping-pong handover. Intercepting satellite data during the 150 to 200 overhead period, it can be seen that the three ping-pong handover rate curves are relatively stable, and the ping-pong handover rate curve will not jitter excessively due to the small total handover times. Comparing the three handover algorithms, it can be seen that the ping-pong handover rate of the handover algorithm based on the elevation angle is about 22%, the ping-pong handover rate of the handover algorithm based on RSRP is about 18%, and the ping-pong handover rate of the handover algorithm based on the reconfigurable factor graph is 12%. Since the satellite beam to the ground power is relatively average, the handover algorithm based on RSRP is likely to cause late handover, so its ping-pong handover rate performance is slightly better than that of the handover algorithm based on elevation angle. The proposed handover algorithm based on a reconfigurable factor graph considers multiple handover factors and is far superior to the other two handover algorithms in terms of ping-pong handover rate performance.

In the same way, the ratio of the number of RLFs to the total number of handovers is the RLF rate. The simulation result graph should take the number of times as the horizontal axis, the failure rate is the vertical axis.

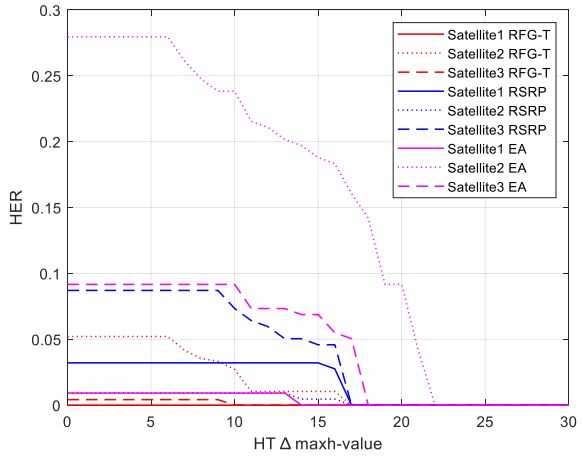

FIGURE 17. Excessive handovers under the different range of the maximum number of tolerance handovers.

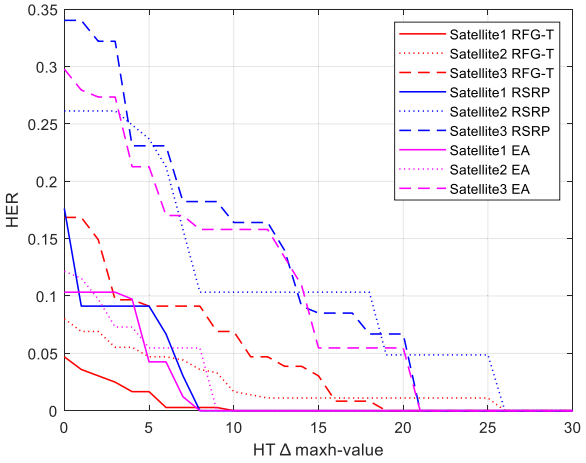

FIGURE 18. Wrong handovers under the different range of the maximum number of tolerance handovers.

Analyzing the RLF rate in Figure 14, we can see the different performances of the three handover algorithms on this indicator. Similarly, to avoid over-jittering in the RLF curve, we intercepted 150 to 200 satellites. Data during the over-the-top period. Comparing the three handover algorithms, it can be seen that the RLF rate of the RSRP-based handover algorithm is about 12%, and the RLF rate of the elevation-based handover algorithm is about 10%. The RLF rate based on the reconfigurable factor graph is about 5.7%. Early handover is mainly based on ping-pong handover, while delayed handover is mainly based on RLF. The performance of the RSRP-based handover algorithm on the ping-pong handover rate is slightly worse than that of the handover algorithm based on the elevation angle on the RLF rate due to the handover algorithm based on the elevation angle. The proposed handover algorithm based on a reconfigurable factor graph also shows better performance in the RLF rate.

We define the handover error rate (HER) as the criteria index of handover performance. HER can be calculated as $\frac{N\_nth}{N}$ or $\frac{N\_hto}{N}$, where, N is the number of all handovers. N_nth is the number of handovers that would not be operated but operated for wrong determinations, N_hto is the number of handovers that would be operated but operated for wrong determinations. In the definition of HER, we have three key parameters: the handover tolerance times maxh, the handover tolerance value HT Δmaxh_value, the range of the maximum number of tolerance handovers maxh_range. In the range of determination, UEs operate RRM and initiate handover requests if the measured number of launch handovers is more than maxh. In this simulation, maxh is configured as 2. After 100 times simulations for different scenarios, the performances of handover by different HT are shown in Figures 15 to 18. When the maxh_range increase, the HER of different HT determinations increases. Figure 15 shows the HER of the handovers which would not be operated but operated for wrong determinations in the case of the same HT $\Delta maxh\_value$.

Figure 16 shows the HER of the handovers which would be operated but operated for wrong determinations in the case of the same HT Δmaxh_value. The HER by RFG-T method is much smaller than those of RSRQ and evaluation methods. When the HT Δmaxh_value increases, the HER of different HT determinations shows a downward trend. Figure 17 shows the HER of the handovers which would not be operated but operated for wrong determinations in the case of the same HT maxh_range. Figure 18 shows the HER of the handovers which would be operated but not operated for wrong determinations in the case of the same HT maxh_range. The HER by RFG-T method is also much smaller than those determined by RSRQ and elevation.

VI. CONCLUSION

In this paper, we proposed a novel method to determine the handover threshold based on a reconfigurable factor graph for the LEO satellite internet network. We designed MFDP determination of HT for SIN. The tensor in the reconfigurable factor graph can be introduced to describe multi-factors with sharp changeable correlations in SIN. To verify the performance of the proposed algorithm, we built a simulation, which showed the proposed HT method has better performance than those of RSRQ and elevation.

REFERENCES

[1] L. Zhang, Y.-C. Liang, and D. Niyato, "6G visions: Mobile ultra-broadband, super Internet-of-Things, and artificial intelligence," *China Commun.*, vol. 16, no. 8, pp. 1–14, Aug. 2019.
[2] C. Sergiou, M. Lestas, P. Antoniou, C. Liaskos, and A. Pitsillides, "Complex systems: A communication networks perspective towards 6G," *IEEE Access*, vol. 8, pp. 89007–89030, 2020.
[3] S. Chen, Y. Liang, S. Sun, S. Kang, W. Cheng, and M. Peng, "Vision, requirements, and technology trend of 6G: How to tackle the challenges of system coverage, capacity, user data-rate and movement speed," *IEEE Wireless Commun.*, vol. 27, no. 2, pp. 218–228, Apr. 2020.
[4] C. Duan, J. Feng, H. Chang, B. Song, and Z. Xu, "A novel handover control strategy combined with multi-hop routing in LEO satellite networks," in *Proc. IEEE Int. Parallel Distrib. Process. Symp. Workshops (IPDPSW)*, May 2018, pp. 845–851.
[5] H. Hu, S. Zhang, and B. Tang, "Leo software defined networking based on onboard controller," in *Proc. IEEE Global Conf. Signal Inf. Process. (GlobalSIP)*, Nov. 2018, pp. 1068–1071.

[6] D. Ding, D.-T. Ma, and J.-B. Wei, "A threshold-based handover prioritization scheme in LEO satellite networks," in *Proc. 4th Int. Conf. Wireless Commun., Netw. Mobile Comput.*, Oct. 2008, pp. 1–6.
[7] Y. Wu, G. Hu, F. Jin, and J. Zu, "A satellite handover strategy based on the potential game in LEO satellite networks," *IEEE Access*, vol. 7, pp. 133641–133652, 2019.
[8] T.-L. Sheu and J.-Y. Sie, "A dynamic adjustment scheme in handover thresholds for off-loading LTE small cells," in *Proc. IEEE Int. Conf. Appl. Syst. Invention (ICASI)*, Apr. 2018, pp. 180–183.
[9] S. Chang, G. Li, J. Zhao, J. Wu, and B. Zhang, "Individualized optimization of handover parameters in 5G (NR) indoor and outdoor co-frequency scenarios," in *Proc. IEEE Int. Conf. Consum. Electron. Comput. Eng. (ICCECE)*, Jan. 2021, pp. 59–66.
[10] M. Anas, F. D. Calabrese, P. E. Mogensen, C. Rosa, and K. I. Pedersen, "Performance evaluation of received signal strength based hard handover for UTRAN LTE," in *Proc. IEEE 65th Veh. Technol. Conf. VTC-Spring*, Apr. 2007, pp. 1046–1050.
[11] A. L. Yusof, M. S. N. Ali, and N. Ya'acob, "Handover implementation for femtocell deployment in LTE heterogeneous networks," in *Proc. Int. Symp. Netw., Comput. Commun. (ISNCC)*, Jun. 2019, pp. 1–5.
[12] J. Xu, Y. Zhao, and X. Zhu, "Mobility model based handover algorithm in LTE-advanced," in *Proc. 10th Int. Conf. Natural Comput. (ICNC)*, Aug. 2014, pp. 230–234.
[13] I. Petrut, M. Otesteanu, C. Balint, and G. Budura, "HetNet handover performance analysis based on RSRP vs. RSRQ triggers," in *Proc. 38th Int. Conf. Telecommun. Signal Process. (TSP)*, Jul. 2015, pp. 232–235.
[14] J. Kurjenniemi, T. Henttonen, and J. Kaikkonen, "Suitability of RSRQ measurement for quality based inter-frequency handover in LTE," in *Proc. IEEE Int. Symp. Wireless Commun. Syst.*, Oct. 2008, pp. 703–707.
[15] S.-U.-R. Qure, S. J. Nawaz, M. Patwary, M. Abdel-Maguid, and A. Kamar, "The impact of propagation environment and velocity on the handover performance of LTE systems," in *Proc. Int. Conf. Wireless Commun. Signal Process. (WCSP)*, Oct. 2010, pp. 1–5.
[16] A. Bottcher and R. Werner, "Strategies for handover control in low Earth orbit satellite systems," in *Proc. IEEE Veh. Technol. Conf. (VTC)*, Jun. 1994, pp. 1616–1620.
[17] E. Papapetrou and F.-N. Pavlidou, "QoS handover management in LEO/MEO satellite systems," *Wireless Pers. Commun.*, vol. 24, no. 2, pp. 189–204, Feb. 2003.
[18] M. Gkizeli, R. Tafazolli, and B. G. Evans, "Hybrid channel adaptive handover scheme for non-GEO satellite diversity based systems," *IEEE Commun. Lett.*, vol. 5, no. 7, pp. 284–286, Jul. 2001.
[19] E. Papapetrou, S. Karapantazis, G. Dimitriadis, and F.-N. Pavlidou, "Satellite handover techniques for LEO networks," *Int. J. Satell. Commun. Netw.*, vol. 22, pp. 231–245, Mar. 2004.
[20] W. Zhao, R. Tafazolli, and B. G. Evans, "Combined handover algorithm for dynamic satellite constellations," *Electron. Lett.*, vol. 32, no. 7, p. 622, 1996.
[21] S. Lembo, S. Horsmanheimo, and M. Laukkanen, "Positioning based intra-frequency handover in indoor cellular network for ultra reliable communications assisted by radio maps," in *Proc. 11th Int. Congr. Ultra Modern Telecommun. Control Syst. Workshops (ICUMT)*, Oct. 2019, pp. 1–9.
[22] Y. Zhao, Z. Chen, H. Su, E. Sun, Y. Guo, and J. Ding, "A position-based secure fast handover mechanism for high-speed trains," in *Proc. IEEE 3rd Int. Conf. Data Sci. Cyberspace (DSC)*, Jun. 2018, pp. 1–6.
[23] T. A. Chowdhury, R. Bhattacharjee, and M. Z. Chowdhury, "Handover priority based on adaptive channel reservation in wireless networks," in *Proc. Int. Conf. Electr. Inf. Commun. Technol. (EICT)*, Feb. 2014, pp. 1–5.
[24] M. Liao, Y. Liu, H. Hu, and D. Yuan, "Analysis of maximum traffic intensity under pre-set quality of service requirements in low earth orbit mobile satellite system for fix channel reservation with queueing handover scheme," *IET Commun.*, vol. 9, no. 13, pp. 1575–1582, Sep. 2015.
[25] S. Wu, K. Y. M. Wong, and B. Li, "A dynamic call admission policy with precision QoS guarantee using stochastic control for mobile wireless networks," *IEEE/ACM Trans. Netw.*, vol. 10, no. 2, pp. 257–271, Apr. 2002.
[26] J. S. Engel and M. M. Peritsky, "Statistically-optimum dynamic server assignment in systems with interfering servers," *IEEE Trans. Veh. Technol.*, vol. VT-22, no. 4, pp. 203–209, Nov. 1973.
[27] D. Li, D. Li, and Y. Xu, "Machine learning based handover performance improvement for LTE-R," in *Proc. IEEE Int. Conf. Consum. Electron. Taiwan (ICCE-TW)*, May 2019, pp. 1–2.
[28] I. Shayea, M. Ergen, A. Azizan, M. Ismail, and Y. I. Daradkeh, "Individualistic dynamic handover parameter self-optimization algorithm for 5g networks based on automatic weight function," *IEEE Access*, vol. 8, pp. 214392–214412, 2020.
[29] T.-L. Sheu and H.-Y. Wang, "A QoS handover scheme with priorities for mobile communications on LTE small cells," in *Proc. 10th Int. Conf. Comput. Intell. Commun. Netw. (CICN)*, Aug. 2018, pp. 6–10.
[30] R. D. Hegazy and O. A. Nasr, "A user behavior based handover optimization algorithm for LTE networks," in *Proc. IEEE Wireless Commun. Netw. Conf. (WCNC)*, Mar. 2015, pp. 1255–1260.
[31] S. Zhang, A. Liu, and X. Liang, "A multi-objective satellite handover strategy based on entropy in LEO satellite communications," in *Proc. IEEE 6th Int. Conf. Comput. Commun. (ICCC)*, Dec. 2020, pp. 723–728.
[32] Z. Wu, F. Jin, J. Luo, Y. Fu, J. Shan, and G. Hu, "A graph-based satellite handover framework for leo satellite communication networks," *IEEE Commun. Lett.*, vol. 20, no. 8, pp. 1547–1550, Aug. 2016.
[33] J. Miao, P. Wang, H. Yin, N. Chen, and X. Wang, "A multi-attribute decision handover scheme for LEO mobile satellite networks," in *Proc. IEEE 5th Int. Conf. Comput. Commun. (ICCC)*, Dec. 2019, pp. 938–942.
[34] C.-Q. Dai, Y. Liu, S. Fu, J. Wu, and Q. Chen, "Dynamic handover in satellite-terrestrial integrated networks," in *Proc. IEEE Globecom Workshops (GC Wkshps)*, Dec. 2019, pp. 1–6.
[35] Y. Su, Y. Liu, Y. Zhou, J. Yuan, H. Cao, and J. Shi, "Broadband LEO satellite communications: Architectures and key technologies," *IEEE Wireless Commun.*, vol. 26, no. 2, pp. 55–61, Apr. 2019.
[36] S. Ji, M. Sheng, D. Zhou, W. Bai, Q. Cao, and J. Li, "Flexible and distributed mobility management for integrated terrestrial-satellite networks: Challenges, architectures, and approaches," *IEEE Netw.*, vol. 35, no. 4, pp. 73–81, Jul. 2021.
[37] M. Kaur and D. Prashar, "Analysis of geographic position mobility oriented routing protocol for FANETs," in *Proc. 9th Int. Conf. Rel., Infocom Technol. Optim. (Trends Future Directions) (ICRITO)*, Sep. 2021, pp. 1–4.
[38] L. Boukhatem, D. Gaiti, and G. Pujolle, "A channel reservation algorithm for handover issues in LEO satellite systems based on a satellite-fixed cell coverage," in *Proc. IEEE VTS 53rd Veh. Technol. Conf., Spring*, May 2001, pp. 2975–2979.
[39] S. Chatterjee, J. Saha, S. Banerjee, and A. Mondal, "Neighbour location based channel reservation scheme for LEO satellite communication," in *Proc. Int. Conf. Commun., Devices Intell. Syst. (CODIS)*, Dec. 2012, pp. 73–76.
[40] F. Vieira, D. E. Lucani, and N. Alagha, "Load-aware soft-handovers for multibeam satellites: A network coding perspective," in *Proc. 6th Adv. Satell. Multimedia Syst. Conf. (ASMS) 12th Signal Process. Space Commun. Workshop (SPSC)*, Sep. 2012, pp. 189–196.
[41] Z. Huan and W. Zunpei, "An INS/GNSS/OD integrated navigation algorithm based on factor graph," in *Proc. IEEE 9th Joint Int. Inf. Technol. Artif. Intell. Conf. (ITAIC)*, Dec. 2020, pp. 2266–2270.
[42] A. Makarau, G. Palubinskas, and P. Reinartz, "Factor graph models for multisensory data fusion: From low-level features to high level interpretation," in *Proc. IEEE Int. Geosci. Remote Sens. Symp.*, Jul. 2012, pp. 162–165.
[43] S. Si, Y. Zhang, L. Luo, and N. Li, "A new underwater all source positioning and Navigation(ASPN) algorithm based on factor graph," in *Proc. Chin. Control Decis. Conf. (CCDC)*, Jun. 2019, pp. 2742–2746.

WENLIANG LIN received the B.S. and Ph.D. degrees in electronic engineering from the Beijing University of Posts and Telecommunications (BUPT), China, in 2010 and 2016, respectively. Currently, he is an Associate Professor with BUPT. He has gained 13 patents from the China Patent Office and has published 14 articles that have been indexed by SCI and EI. He also participated in three National High Technology Research and Development Programs ("863"Program) of China. His research interests include 6G and satellite mobile communications.

YILIE HE received the B.S. degree from Hangzhou Dianzi University, in 2020. Currently, he is pursuing the master's degree with the School of Electronic Engineering, Beijing University of Posts and Telecommunications (BUPT), China. His research interests include satellite communication and 5G/6G communication.

KE WANG received the Ph.D. degree in electronic engineering from the Beijing University of Posts and Telecommunications (BUPT), China, in 2014. Since 2014, he has been an Assistant Professor with the BUPT, where he is currently an Associate Professor.

ZHONG-LIANG DENG (Senior Member, IEEE) received the B.S. degree from the Beijing University of Aeronautics and Astronautics, in 1991, and the Ph.D. degree from Tsinghua University, Beijing, China, in 1994. Since 1996, he has been a famous Professor at the Beijing University of Posts and Telecommunications (BUPT). He is the top future indoor navigation expert in China. He has gained 56 patents from the China Patent Office and has published 213 articles indexed by the SCI and EI. He has participated in the National High Technology Research and Development Program (''863''Program) of China. He has also received two National Science and Technology Progress Awards in China.

DONGDONG WANG received the Ph.D. degree in information and communication engineering from the Beijing University of Posts and Telecommunications (BUPT), in 2018. He is currently a Senior Engineer and a Young Expert in the field of LEO satellite transmission technology with the Science and Technology on Communication Networks Laboratory, Network Communication Research Institute, China Electronics Technology Group Corporation. He has authored or coauthored over 20 technical articles in international journals and conferences. His research interests include information theory and channel coding, and 5G-based LEO satellite transmission technology.

XIAOYI YU is currently pursuing the Ph.D. degree with the School of Electronic Engineering, Beijing University of Posts and Telecommunications, China. Her research interests include satellite communication, 5G/6G communication, resource management, and random access.

YANG LIU received the B.S. degree in communication engineering from the Chongqing University of Posts and Telecommunications, in 2016. He is currently pursuing the Ph.D. degree with the Department of Electrical Engineering, Beijing University of Posts and Telecommunications, Beijing, China. His research interests include 6G and satellite mobile communications.

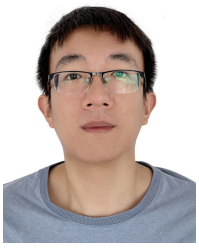

HAO LIU received the B.S. degrees from Hangzhou Dianzi University, Hangzhou, China, in 2013 and 2017, respectively. He is currently pursuing the Ph.D. degree with the School of Electrical Engineering, Beijing University of Posts and Telecommunications, China. His research interests include satellite communication, 5G communication, and machine learning.

LEI GU received the B.S. degree from Zhengzhou University, in 2019. Currently, he is pursuing the master's degree with the School of Electronic Engineering, Beijing University of Posts and Telecommunications (BUPT), China. His research interests include satellite communication and 5G/6G communication.

BINGYU XU received the B.Sc. degree in telecommunications engineering with management from the Beijing University of Posts and Telecommunications, China, and the Ph.D. degree in electronic engineering from the Queen Mary University of London, London, U.K. She is currently a Senior Engineer of information and communication engineering with the China Academy of Information and Communications Technology. She has published 14 articles, in which two are indexed by SCI and eight indexed by EI. She is the author of the book *Multiple Access Techniques for 5G Wireless Networks and Beyond* and has gained two patents. Her current research interests include wireless networks and satellite communication.